OXFORD GENETICS

GENETICS, 2023, 224(4), iyad104
https://doi.org/10.1093/genetics/iyad104
Advance Access Publication Date: 1 June 2023
Brief Investigation

Mob4 is essential for spermatogenesis in *Drosophila melanogaster*

Inês B. Santos,[1,2,3] Alan Wainman,[4] Juan Garrido-Maraver,[1,2,3,5] Vanessa Pires,[1,2,3] Maria Giovanna Riparbelli,[6] Levente Kovács,[7] Giuliano Callaini,[6] David M. Glover,[7] Álvaro A. Tavares[1,2,3,*]

[1]Faculty of Medicine and Biomedical Sciences, University of Algarve, 8005-139 Faro, Portugal
[2]Centre for Biomedical Research (CBMR), University of Algarve, 8005-139 Faro, Portugal
[3]Algarve Biomedical Center (ABC), University of Algarve, 8005-139 Faro, Portugal
[4]Sir William Dunn School of Pathology, University of Oxford, South Parks Road, Oxford, OX1 3RE, UK
[5]Centro Andaluz de Biología del Desarrollo, Universidad Pablo de Olavide, 41013 Sevilla, Spain
[6]University of Siena, Department of Life Sciences, Via Aldo Moro, 2, 53100 Siena, Italy
[7]Division of Biology and Biological Engineering, California Institute of Technology, 91125 Pasadena, California

*Corresponding author: Email: aatavares@ualg.pt

Abstract

Gamete formation is essential for sexual reproduction in metazoans. Meiosis in males gives rise to spermatids that must differentiate and individualize into mature sperm. In *Drosophila melanogaster*, individualization of interconnected spermatids requires the formation of individualization complexes that synchronously move along the sperm bundles. Here, we show that Mob4, a member of the Mps-one binder family, is essential for male fertility but has no detectable role in female fertility. We show that Mob4 is required for proper axonemal structure and its loss leads to male sterility associated with defective spermatid individualization and absence of mature sperm in the seminal vesicles. Transmission electron micrographs of developing spermatids following mob4^{RNAi} revealed expansion of the outer axonemal microtubules such that the 9 doublets no longer remained linked to each other and defective mitochondrial organization. Mob4 is a STRIPAK component, and male fertility is similarly impaired upon depletion of the STRIPAK components, Strip and Cka. Expression of the human Mob4 gene rescues all phenotypes of *Drosophila mob4* downregulation, indicating that the gene is evolutionarily and functionally conserved. Together, this suggests that Mob4 contributes to the regulation of the microtubule- and actin-cytoskeleton during spermatogenesis through the conserved STRIPAK complex. Our study advances the understanding of male infertility by uncovering the requirement for Mob4 in sperm individualization.

Keywords: Mob4, axoneme, spermiogenesis, male fertility, STRIPAK complex

Introduction

The many causes of male infertility include defects in spermatogenesis. However, there is still limited knowledge of the molecular and cellular processes that regulate sperm production and that lead to its failure in humans (Tüttelmann *et al.* 2018). *Drosophila melanogaster* offers a powerful model in which to uncover genes that execute and regulate spermatogenic processes, and many of the genes involved in spermatogenesis in *Drosophila* are conserved in humans (White-Cooper 2010; Siddall and Hime 2017).

In *Drosophila* testes, cysts of 16 primary spermatocytes undertake meiosis to generate cysts of 64 syncytial haploid spermatids (reviewed in Fuller 1998). Cells within each cyst are interconnected by cytoplasmic bridges due to incomplete cytokinesis (Lin *et al.* 1994). The synchronous differentiation of spermatids within each cyst requires formation of flagellar axonemes and acrosomes, remodeling of mitochondria and nuclei, accompanied by elongation of the developing sperm and their plasma membranes (Tates 1971; Lindsley and Tokuyasu 1980). The fully elongated syncytium of 64 spermatids then undergoes a membrane remodeling process known as individualization, which requires that actin cones form around each of the 64 nuclei that assemble into an individualization complex (IC) (Fuller 1998). The IC moves processively along the spermatid bundle, stripping away unnecessary organelles and cytoplasm, forming the "cystic bulge" (Tokuyasu *et al.* 1972) and so remodeling the cyst membrane and resolving intercellular bridges in order that each sperm cell becomes encased in its own plasma membrane (Fabrizio *et al.* 1998). By the end of the individualization process, the cystic bulge is disposed of in the "waste bag" in a caspase-dependent apoptosis-like event, leaving the now fully individualized mature sperm.

The striatin-interacting phosphatase and kinase (STRIPAK) complex is an evolutionarily conserved supramolecular complex with functions in cell proliferation, migration, vesicular transport, cardiac development, and immune regulation (Goudreault *et al.* 2009; Hwang and Pallas 2014; Neisch *et al.* 2017). Although many isoforms and paralogs of STRIPAK subunits can assemble into various STRIPAK variants, the core STRIPAK complex of *Drosophila* includes striatin (Cka), protein phosphatase 2A (Pp2A-29B, Mts), protein kinase (Gck-III), and regulatory and structural subunits (Strip, Mob4). These core subunits are structurally

Received: March 02, 2023. **Accepted:** May 17, 2023

conserved in all eukaryotes. In *Drosophila* and mammals, STRIPAK complexes act as platforms to integrate upstream inputs to the Hippo pathway (Chen *et al.* 2019). Several STRIPAK components have been reported to suppress Hippo signaling, thereby regulating cell proliferation (Couzens *et al.* 2013; Bae *et al.* 2017; Zheng *et al.* 2017).

Mob4 can inactivate the Hippo pathway as a core component of STRIPAK complex, resulting in enhanced expression of growth-promoting genes (Chen *et al.* 2018). Mob4 also regulates neurogenesis and synapse formation (Baillat *et al.* 2001; Florindo *et al.* 2023) and is required for both centrosome separation and focusing of kinetochore fibers (Trammell *et al.* 2008). Within the STRIPAK complex, Mob4 acts as a molecular glue to tether STRN1 (the mammalian homolog of Cka) to the main body of STRIPAK. Mob4 point mutations targeting phospho-threonine binding sites to Strip1 (the mammalian homolog of Strip), decrease the formation of STRIPAK, leading to deregulated Hippo signaling (Jeong *et al.* 2021).

Here, we report an essential role for Mob4 in spermatogenesis in *D. melanogaster* and show that the human Mob4 homolog can rescue the *Drosophila* phenotypes, indicating conserved molecular function.

Materials and methods

Fly husbandry and genetics

All *Drosophila* stocks used in this study were maintained on standard cornmeal–yeast–sucrose media and are listed in Supplementary Table 1. Unless otherwise indicated, experiments were performed at 25°C. The w^{1118} flies were used as wild-type strain. The $mob4^{P}$ mutant allele was generated using the *P*-element remobilization technique, in the line y; KG4509 P[$y^{mDint2}w^{+}$ BR.E.BR = SUPor-P] (Gene Disruption Project, Bellen *et al.* 2004). The $mob4^{SVC}$ mutant allele was generated by CRISPR/Cas9-catalyzed homology-directed repair by the sgRNA pair targeted by 5′-GGATCATCGCGTCTTCGAGC-3′ and 5′-GCGAGT CTGACTAATCTGGG-3′ sequences (Gratz *et al.* 2014).

Tissue-specific genetic manipulation

For early germ cell-specific gene depletion, flies carrying the *nanos* (*nos*)*-GAL4:VP16* or *bam-GAL4:VP16* were crossed to flies carrying dsRNA under UAS control. Control flies were the progeny of the cross between the driver and *UAS-mCherry*^{RNAi}.

Viability assay

Ubiquitous depletion was accomplished by crossing flies carrying the daughterless (*da*)*-GAL4* driver with flies carrying dsRNA against the genes of interest. Each cross was established with 5 virgin females (aged 1–3 days) and 5 age-matched males. Mating was allowed for 3 days, and then flies were discarded. The number of pupae and the number of eclosed adults were scored in 6 independent crosses, and viability is expressed as the percentage of flies that eclosed from the pupae.

Fertility assay

To test female fertility, virgin female flies (aged 1–3 days) depleted for the genes of interest (see *tissue-specific genetic manipulation*) were collected and individually mated with 2 wild-type age-matched males. The crosses were kept at 25°C for 6 days, after which the adults were removed. The number of eclosed progeny in each vial was scored. Male fertility was similarly tested as described; individual males depleted for the genes of interest were mated with 2 wild-type virgin females. Vials in which any of the adults died were discarded. Ten crosses per genotype were evaluated in 2 independent experiments.

Statistical analysis

The sample size (n), mean, SEM, and number of times each experiment was repeated (N) are indicated in corresponding figure legends. Data collected from viability and fertility assays were analyzed with a 2-tailed, unpaired *t*-test by GraphPad Prism version 7.03 for Windows. *P*-values for each analysis are indicated in corresponding figure legends; a 99% confidence interval was applied in all statistical tests.

Immunostaining of *whole-mount testes*

Testes from unmated young adults (2-day-old males unless otherwise indicated) were fixed in 4% formaldehyde/ phosphate-buffered saline (PBS) for 20–30 min. Samples were washed 3 times in PBST for 20 min, and blocked in PBST/10% SFB/10% BSA for 1 h. The samples were incubated overnight in a humid chamber at 4°C with the following primary antibodies: mouse anti-pan polyglycylated tubulin (1:1000, Axo-49; Sigma) and rabbit anti-cleaved caspase 3 (1:500, Cell Signaling #9661). DNA and actin were stained with 1 µg/mL DAPI and phalloidin (1:1000, Flash Phalloidin™ Red 594; BioLegend).

Confocal microscopy

Images were acquired on a LSM710 confocal microscope (Zeiss). All processing and analysis of microscope images was performed with ImageJ 1.53q (Schneider *et al.* 2012). Figures were created using the QuickFigures2 plugin for FIJI/ImageJ (Mazo 2021).

Transmission electron microscopy

Testes from control and $mob4^{RNAi}$ young males were dissected in PBS pH 7.2, and fixed in 2.5% glutaraldehyde in PBS overnight at 4°C. Samples were then fixed in 1% osmium tetroxide in PBS for 1–2 h at 4°C and dehydrated through a graded series of ethanol, infiltrated with a mixture of Epon-Araldite resin and polymerized at 60°C for 48 h. Silver-gray sections (70-nm thick) were cut and stained with 2% aqueous uranyl acetate for 20 min in the dark and then with lead citrate for 2 min. TEM preparations from control (n = 11) and mob4^{RNAi} (n = 14) males were observed with a Tecnai G2 Spirit EM equipped with an Osis Morada CCD camera.

GFP-Trap affinity purification

The 0–2 h embryos expressing *GFP-only* (negative control) or *GFP-mob4* were dechorionated and snap-frozen in liquid nitrogen. The protocol for affinity purification of protein complexes from *Drosophila* embryos was previously published (Lipinszki *et al.* 2014). Isolated proteins were digested with trypsin, and the resulting peptide samples were analyzed using an Orbitrap-LTQ mass spectrometer (Thermo Fisher Scientific). Acquired data were searched using the Mascot program (Matrix Science) against the *D. melanogaster* database.

Results

Lack of *mob4* causes lethality and male sterility in *D. melanogaster*

To study the potential functions of the *mob4* gene, we generated 2 different *mob4* mutant alleles (Fig. 1a). The first, $mob4^{P}$, generated by *P*-element mutagenesis, lacks most of the first exon, including the start codon. Homozygous $mob4^{P}$ animals died during the third larval *instar* stage, but when heterozygous against a deficiency ($mob4^{P}/Df$), adult male flies were formed that were sterile whereas

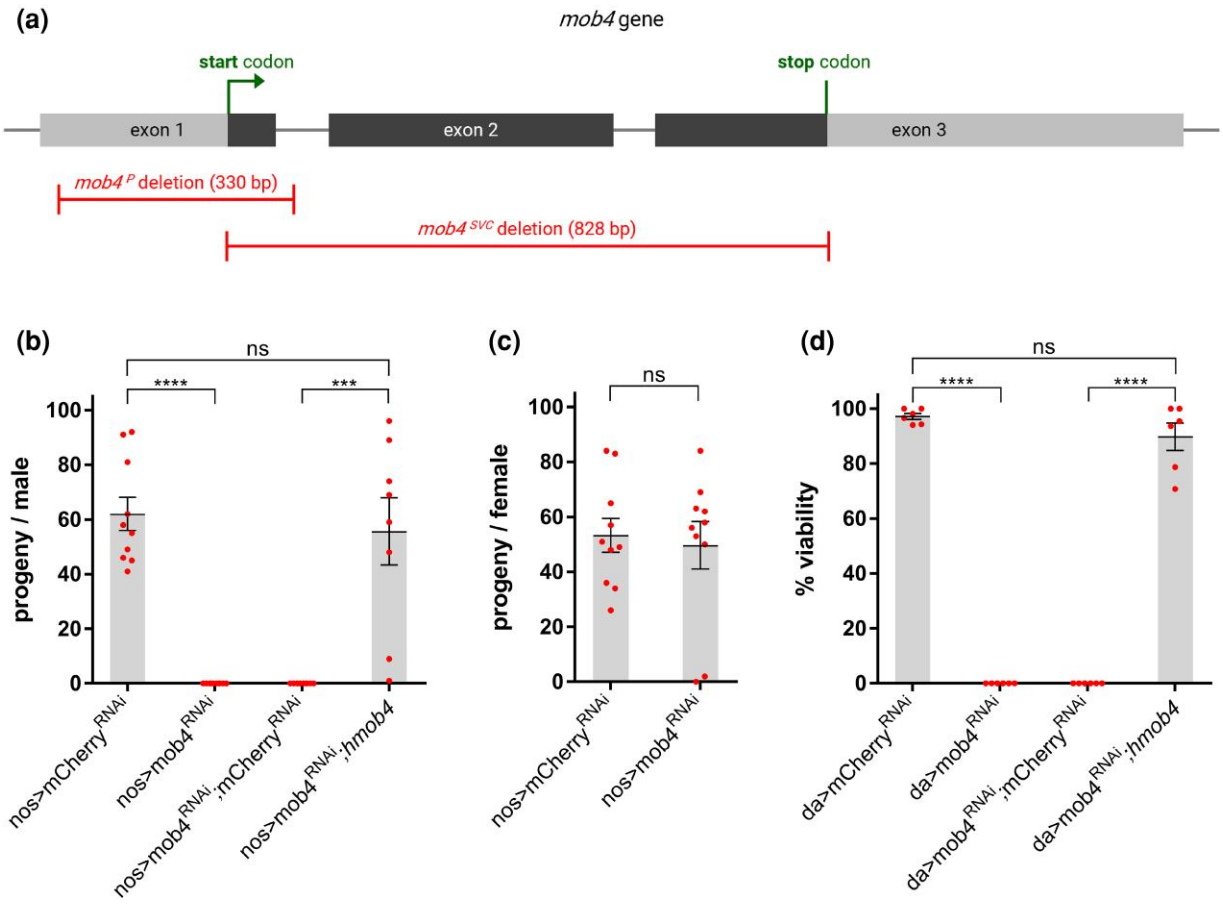

Fig. 1. Mob4 is essential for viability and male fertility in *Drosophila melanogaster*. a) Schematic of Mob4 gene and mutant alleles (red). The $mob4^{P}$ deletion allele was generated by imprecise excision of the *P*-element in the line KG4509, and the $mob4^{SVC}$ deletion allele was generated by CRISPR/Cas9-targeted mutagenesis. The endpoints of deletion in $mob4^{P}$ and $mob4^{SVC}$ were determined by sequencing and are indicated in basepairs (bp). b) Male fertility test of control ($mCherry^{RNAi}$), $mob4^{RNAi}$ and rescued flies ($mob4^{RNAi}$ and *hmob4*, both under UAS control). Males of each genotype were individually mated with wild-type females. Data points represent number of progeny from individual males. Means ± SEM are shown for at least $n = 8$ males per genotype. *P*-values of 2-tailed unpaired *t*-tests are indicated (99% confidence level); $^{****}P < 0.0001$, $^{***}P < 0.001$, ns, not significant. c) Fertility test of control and $mob4^{RNAi}$ females. Females of each genotype were individually mated with wild-type males. Data points represent numbers of progeny from individual females. Means ± SEM are shown for $n = 10$ females per genotype. *P*-values of 2-tailed unpaired *t*-tests are indicated (99% confidence level). d) Viability of control, $mob4^{RNAi}$ and rescued flies (as in b). Data points represent percentage of viable flies in 6 independent experiments. The da-GAL4 driver was crossed either to UAS-$mCherry^{RNAi}$ ($n = 439$), UAS-$mob4^{RNAi}$ ($n = 338$), UAS-$mob4^{RNAi}$; UAS-$mCherry^{RNAi}$ ($n = 201$), or UAS-$mob4^{RNAi}$; UAS-*hmob4* ($n = 286$). Means ± SEM are shown. *P*-values of 2-tailed unpaired *t*-tests are indicated (99% confidence level).

the adult females were fertile. Thus, the mutagenized chromosome carries a second site lethal mutation and loss of the N-terminal part of Mob4 results in male sterility. The second *mob4* mutant allele ($mob4^{SVC}$) lacks the entire coding region and showed third *instar* lethality when homozygous or heterozygous to a deficiency lacking *mob4*. The lethality of $mob4^{SVC}$ flies can be rescued by ubiquitous expression of wild-type *GFP-mob4*, indicating that the lethality is a consequence of the mutation in *mob4*.

Intrigued by the sterility of $mob4^{P}/Df$ males, we sought to analyze the role of *mob4* during spermatogenesis. To this end, we used 2 transgenic UAS-$mob4^{RNAi}$ lines in which *mob4* was downregulated in the male germline by 2 different drivers: *nos-GAL4*, which induces target expression in germinal stem cells and spermatogonia, and *bam-GAL4*, which acts in late spermatogonia and early spermatocytes. Identical results were obtained for both UAS-$mob4^{RNAi}$ lines with both drivers, and therefore we present only the results obtained with the *nos-GAL4* driver. Downregulation of *mob4* in the male germline (hereafter $mob4^{RNAi}$) also resulted in male sterility (Fig. 1b), while depletion in the female germline had no effect on fertility (Fig. 1c), thus recapitulating the $mob4^{P}/Df$ phenotype. Ubiquitous depletion of *mob4* resulted in complete lethality at the late larval/pupal stage, phenocopying the *mob4* null mutant phenotype (Fig. 1d). Together, these results indicate that *mob4* is required for male fertility, but not for female fertility.

We found that all phenotypes of *mob4* depletion could be rescued by provision of human *MOB4* (*hmob4*, HGNC:17261) (Fig. 1), which is resistant to dsRNA directed against the *Drosophila* gene, indicating that the lethality and male sterility phenotypes observed upon $mob4^{RNAi}$ are not off-target responses.

Mob4 is required for spermatid individualization

To explore the mechanisms underlying the sterility phenotype, we visualized spermatid axonemes by immunostaining in testes from 2-day-old $mob4^{RNAi}$ males. In control testes, axonemes could be observed throughout the testes length (elongated cysts), in the terminal epithelium (cyst coiling) and inside the seminal vesicles (where mature sperm is stored until mating) (Fig. 2a). By contrast, cysts of $mob4^{RNAi}$ testes were fully elongated, but their seminal vesicles were empty (Fig. 2d). In addition, most of the $mob4^{RNAi}$ sperm bundles accumulated in the terminal epithelium and showed increased accumulation of coiled cysts. On the other

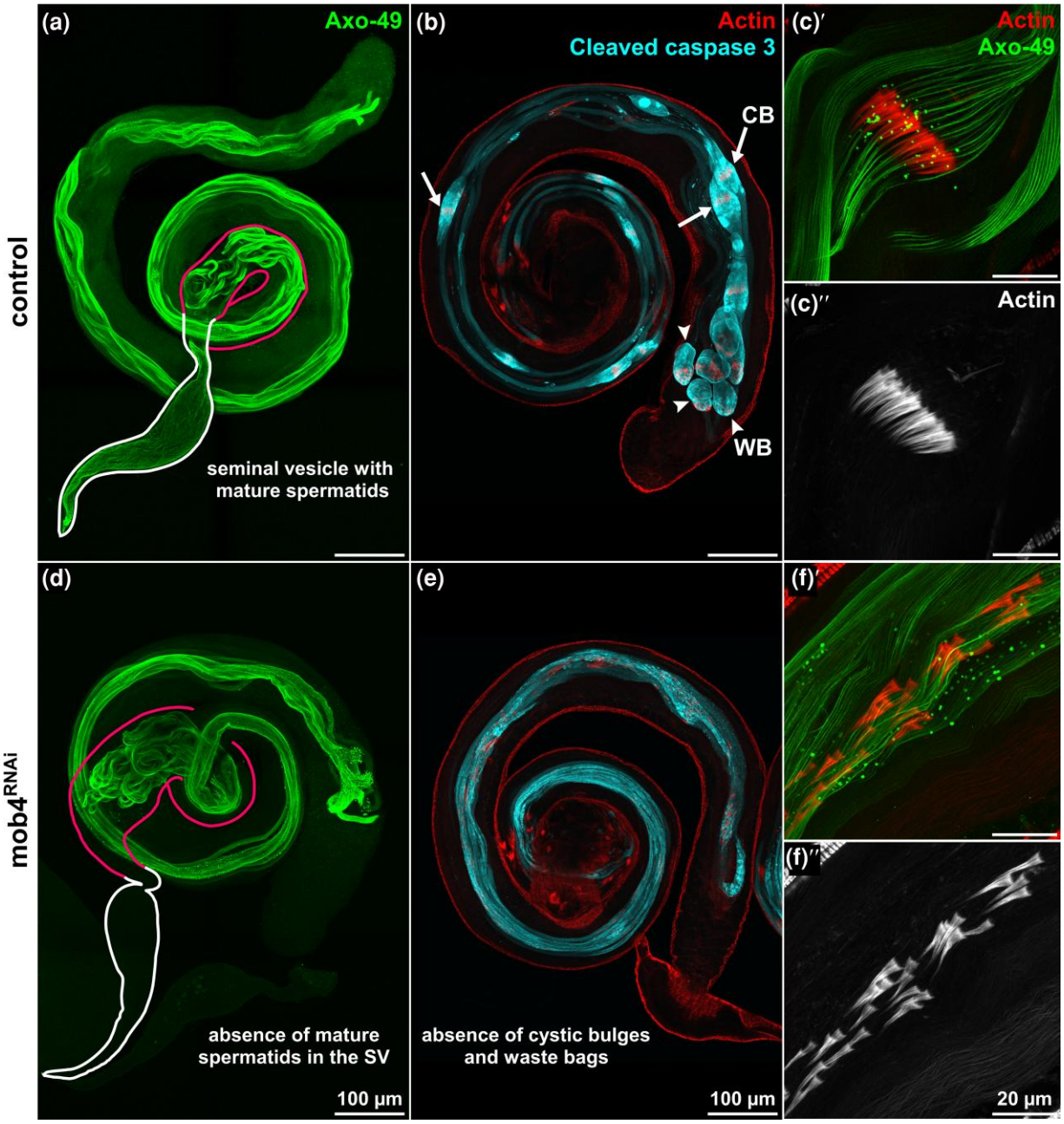

Fig. 2. Individualization defects in *mob4* depleted testes. Control (*mCherry*^{RNAi}) (a) and *mob4*^{RNAi} (d) testes from 2-day-old males were immunostained with antipolyglycylated tubulin (green) to visualize axonemes in individualizing/coiling cysts or mature sperm. The seminal vesicle (SV) and terminal epithelium (TE) are highlighted in white and pink, respectively. Control (b) and *mob4*^{RNAi} (e) testes were stained with phalloidin-594 and immunostained to reveal cleaved caspase 3 (cyan). Cystic bulges (CB, white arrows) and waste bags (WB, white arrowheads) resulting from spermatid individualization can be seen in control testes (b–c) but are absent from *mob4*-depleted testes (e–f). Actin cones and spermatid bundles from control (c) and *mob4*^{RNAi} (f) testes visualized with phalloidin-594 and immunostained to reveal polyglycylated tubulin (green).

hand, nuclear morphology appears to be normal at the round, canoe, and needle stage in mob4^{RNAi} spermatids, suggesting that both nuclear condensation and remodeling progress normally (Supplementary Fig. 1).

Spermatid individualization occurs in the final stage of spermiogenesis and is mediated by ICs (Lindsley and Tokuyasu 1980; Fuller 1993). The actin cones appeared to associate normally with spermatid nuclear bundles in mob4^{RNAi} animals (Supplementary Fig. 1). However, whereas in control testes, the distribution of actin cones suggested uniform movement along the sperm bundles forming the cystic bulge (Fig. 2c), in *mob4*^{RNAi} testes, actin cones were scattered along the sperm bundles suggesting loss of migration synchrony (Fig. 2f) and a failure of individualization.

As multiple caspases and caspase regulators act in nonapoptotic roles to mediate spermatid individualization (Arama *et al.* 2003), we looked whether effector caspases become activated in *mob4*^{RNAi} testes by immunostaining with anticleaved caspase-3 (CC3). In control testes, CC3 signal was mostly restricted to the cystic bulge and the waste bags (Fig. 2b). By contrast, there were neither cystic bulges nor waste bags in *mob4*^{RNAi} testes, although there was caspase activation throughout the whole length of the spermatid tail (Fig. 2e).

Together, these results suggest that in the absence of Mob4, cyst elongation occurs, but disruption of the ICs prevents spermatid individualization and migration of sperm into the seminal vesicle.

Axoneme disruption following *mob4*^{RNAi}

To determine defects in spermiogenesis that might underlie the failure of spermatid individualization in *mob4*^{RNAi} males, we examined the ultrastructure of the developing axoneme in 2-day-old males by transmission electron microscopy (TEM). During the elongation phase, the developing axoneme and major and minor mitochondrial derivatives of wild-type spermatids are encompassed by a plasma membrane, known as the ciliary sheath (Fig. 3a) (Fabrizio *et al.* 1998). The major mitochondrial derivative is filled with an electron dense material of the paracrystalline body. The elongation of the 2 mitochondrial derivatives is required for the elongation and function of the flagellum (Tates 1971; Noguchi *et al.* 2011).

We found that the elongating cysts of *mob4*^{RNAi} males displayed defects in axonemal structure before spermatid individualization was initiated. These defects included the loss of microtubule doublets (Fig. 3b) or preservation of stereotypical 9 + 2 microtubule-doublets of the axoneme but with radial expansion (Fig. 3c). Such abnormal axonemes were typically associated with mitochondrial derivatives of abnormal shape and/or size. Moreover, we also observed elongating spermatid cysts containing 2 paracrystalline body-filled mitochondrial derivatives paired with 1 axoneme, as well as elongating cysts with multiple axonemes and an irregular number of mitochondrial derivatives (Fig. 3d) suggesting an incomplete second meiotic division. Taken together, these findings suggest a role for Mob4 in the structural maintenance of axonemes and in forming or maintaining the integrity of associated cellular structures during spermatogenesis.

GFP-mob4 has a dynamic localization throughout spermatogenesis

Next, we examined the subcellular localization of *GFP-mob4* in testes of 2-day-old males. The rescue of all mutant phenotypes by ubiquitous expression of a *GFP-mob4* transgene indicates that the *GFP-mob4* fusion protein is fully functional. Using *GFP-mob4* transgenic flies, we observed that in meiotically dividing spermatocytes, *GFP-mob4* had a reticular localization accumulating in membranous fibers surrounding the meiotic spindle (Fig. 4c). During individualization, *GFP-mob4* accumulated in the cystic bulge (Fig. 4b). In early canoe stage spermatids, *GFP-mob4* strongly accumulated in individual puncta at the basal side of nuclei in the vicinity of the basal body (Fig. 4d). This punctate localization appeared to be transient as it was absent when the actin cone was forming in spermatids at the late canoe stage (Supplementary Fig. 2). This dynamic behavior of Mob4 at different stages of spermiogenesis suggests a functional requirement for Mob4 in the parafusorial membranes or structures derived from or associated with them, at the basal body or transition zone in the initiation of axoneme elongation, and in the cystic bulge during individualization per se.

Strip and Cka are required for spermatid individualization

We affinity-purified *GFP-mob4* from *Drosophila* syncytial embryos and analyzed the complexes by mass spectrometry; samples

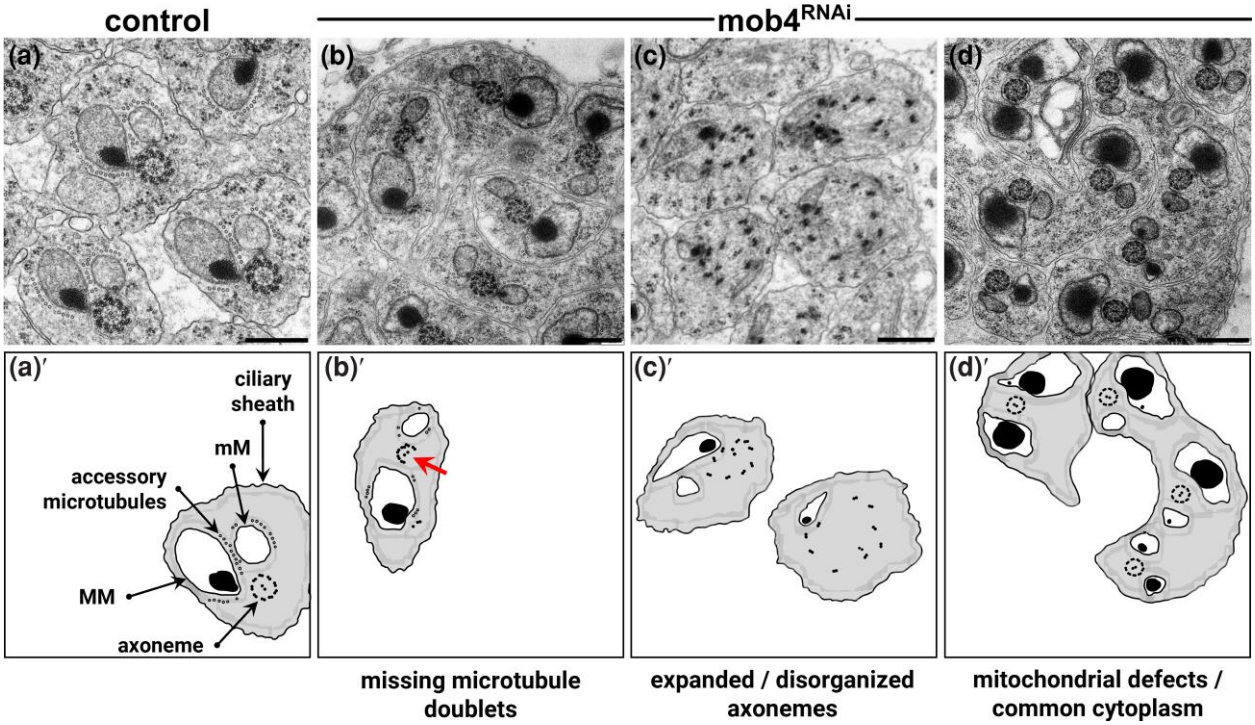

Fig. 3. Electron microscopy reveals aberrant axonemal structure and mitochondrial defects in *mob4* depleted spermatid cysts. a) Transverse section of control (*mCherry*^{RNAi}) elongating spermatids showing the major mitochondrial derivative (MM) containing paracrystalline material and the minor mitochondrial derivative (mM) adjacent to the axoneme. Accessory microtubules are in the vicinity of the mitochondrial derivatives. b) *mob4*^{RNAi} spermatids with incomplete axonemes (red arrow points to missing microtubule doublets). c) *mob4*^{RNAi} spermatids with "expanded" axonemes showing loss of linkage between microtubule doublets. d) *mob4*^{RNAi} spermatids sharing the same ciliary sheath and spermatids where both mitochondrial derivatives accumulate paracrystalline material. (a'–d') shows the schematic representation of (a–d). Scale bar represents 500 nm.

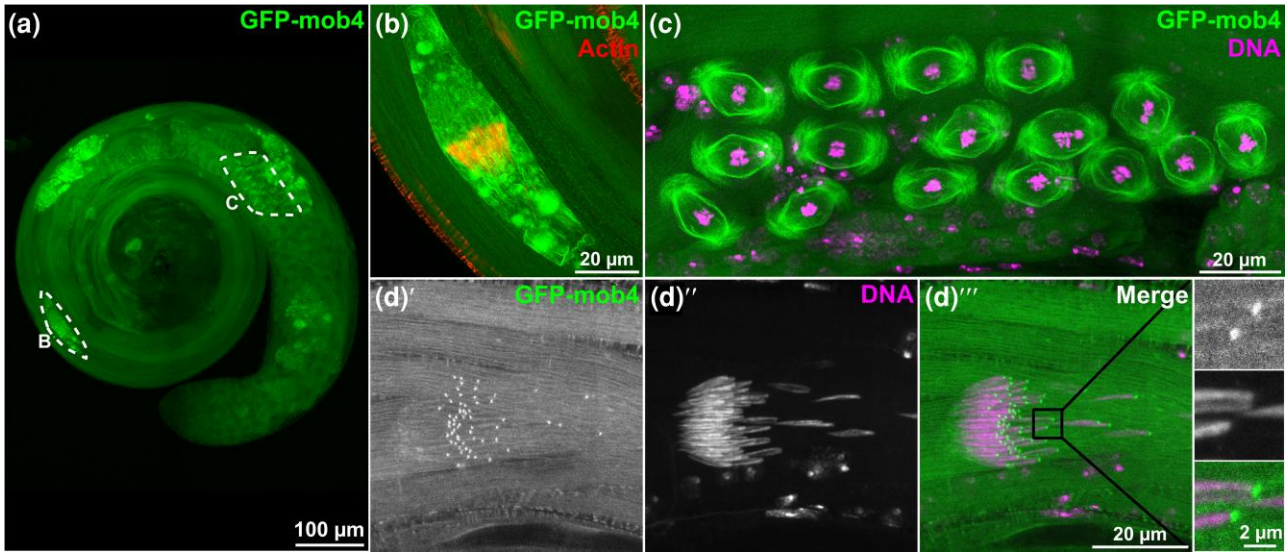

Fig. 4. *GFP-mob4* localization throughout spermatogenesis. a) Testes from 2-day-old males expressing *GFP-mob4* were stained to reveal DNA (DAPI stain, in magenta), actin cones (phalloidin-594, in red) and fluorescence of *GFP-mob4* (green) (b) *GFP-mob4* accumulates in the cystic bulge surrounding actin cones in individualizing spermatid bundles. c) *GFP-mob4* has a reticular localization around the parafusorial membranes and associated with microtubules during the meiotic divisions. d) *GFP-mob4* (d') localizes to the basal end of the nuclei (d'') in early canoe stage spermatids (see also Supplementary Fig. 2).

prepared from embryos expressing *GFP* alone were used as a negative control to exclude proteins that either bind to the GFP-tag or to the beads themselves. This approach identified STRIPAK core components as the interactants with highest Mascot scores (Supplementary Table 2). We therefore questioned whether knockdown of STRIPAK core components might replicate the $mob4^{RNAi}$ phenotypes. We found that ubiquitous depletion of either *Strip* or *Cka*, via RNAi, induced late larval/pupal lethality (Fig. 5a) as previously described for mutant alleles of these loci (Chen *et al.* 2002; Sakuma *et al.* 2014). When we downregulated *Strip* and *Cka* in the *Drosophila* germline, we found that depletion of *Strip* resulted in 100% male sterility while depletion of *Cka* led to ~50% of males being sterile (Fig. 5b). Curiously, only $Strip^{RNAi}$ had any impact on female fertility, with progeny dropping to a third of control levels (Fig. 5c).

Testes from 2-day-old $Strip^{RNAi}$ males revealed scattered actin cones and no mature sperm accumulating in the seminal vesicle (Fig. 5j-k). As control animals aged, their seminal vesicles increased in volume, due to continued sperm accumulation (Fig. 5d/g). However, the seminal vesicles of either 10-day-old $mob4^{RNAi}$ (Fig. 5e/h) or $Strip^{RNAi}$ (Fig. 5f/i) males failed to fill with sperm, and no increase in volume was observed. Instead, there was enlargement of the terminal epithelium suggestive of continuous production of aberrant sperm and abnormal sperm coiling. Testes from Cka^{RNAi} males showed both mature sperm in the seminal vesicle and abnormal enlargement of the terminal epithelium. Accordingly, we could detect some intact ICs, but the great majority of the actin cones were scattered (Fig. 5l-m). We conclude that, like Mob4, Strip and Cka are required for sperm individualization and male fertility.

Discussion

Here, we describe a previously unknown function of Mob4 in spermatid differentiation. *Mob4* depleted testes undertake cyst elongation after meiosis, but spermatids fail to individualize and the seminal vesicles are devoid of mature sperm. Our results accord with the testes being the tissue with highest levels of Mob4 expression (FlyAtlas2) (Krause *et al.* 2022).

One primary defect of spermiogenesis in *mob4*-depleted testes is the loss of the structural integrity of the axoneme. Spermiogenesis requires intense cytoskeletal reorganization, not only of microtubules in axoneme elongation but also with actin having a major role in spermatid individualization (Lindsley *et al.* 1980; Fabrizio *et al.* 1998). Several mutants for microtubule-binding proteins have been shown to affect the axoneme structure and lead to individualization defects. For example, testes mutant for Bug22, a conserved protein that associates with basal bodies and cilia, shows defects in sperm individualization characterized by disrupted spermatid axonemes (Maia *et al.* 2014). Flies depleted for TTLL3B, an essential member of the tubulin tyrosine ligase-like family, are male sterile with either missing axonemes or axonemes composed of singlet microtubules and having sperm individualization defects (Rogowski *et al.* 2009). To our knowledge, however, "expanded" axonemes having all 9 outer doublets but with complete loss of linkage between doublets is a unique characteristic of *mob4* downregulation. It is possible that the short-lived presence of *GFP-Mob4* at the basal body may correlate with such defects, but this would require further studies.

Previous genetic studies have shown Mob4 to be a regulator of microtubule organization and axonal transport in *Drosophila* neurons (Schulte *et al.* 2010), and to play roles in the microtubule-based mitotic spindles in cultured cells (Baillat *et al.* 2001). Moreover, in zebrafish and nematodes, *mob4* mutants have defective microtubule networks, and Mob4 interacts directly with the tubulin- and actin-folding TRiC/CCT chaperone complex (Khabirova *et al.* 2014; Berger *et al.* 2022). We also identified components of the TRiC/CCT complex as molecular partners of *GFP-Mob4* (Supplementary Table 2). In the light of these findings, it is tempting to suggest that the spermatogenesis defects we now report when downregulating *mob4* are due to impaired microtubule function.

Our finding that downregulation of either *Strip* or *Cka* results in similar failures of sperm individualization to Mob4 suggests that this process requires the STRIPAK complex. Strip and Cka were

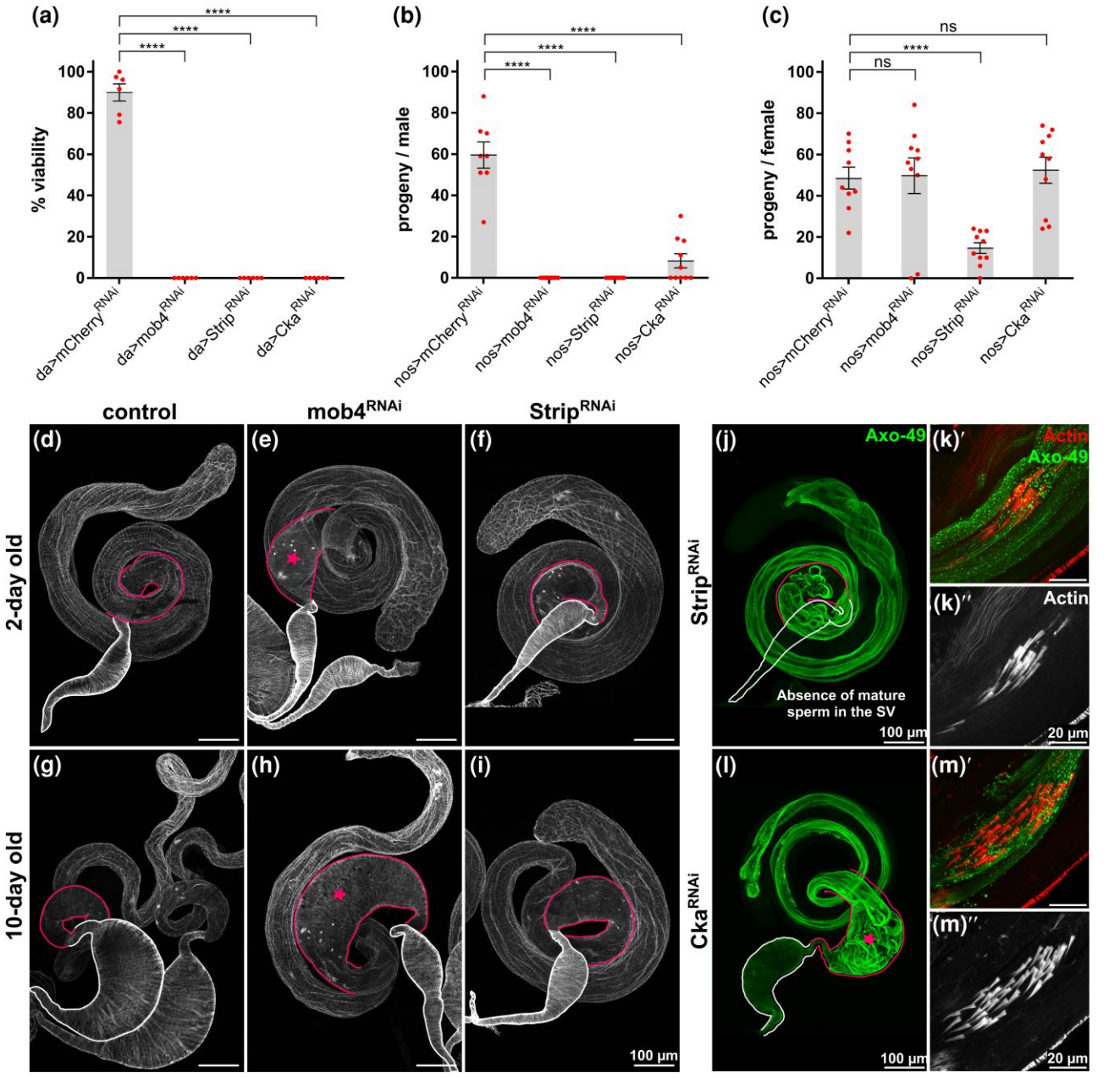

Fig. 5. STRIPAK components Mob4, strip, and Cka are required for male fertility in *Drosophila melanogaster*. a) Viability of control (*mCherry*^{RNAi}), *mob4*^{RNAi}, *Strip*^{RNAi}, and *Cka*^{RNAi}. Data points represent percentage of viable flies in 6 independent experiments. The da-GAL4 driver was crossed either to UAS-*mCherry*^{RNAi} ($n = 417$), UAS-*mob4*^{RNAi} ($n = 266$), UAS-*Strip*^{RNAi} ($n = 244$), or UAS-*Cka*^{RNAi} ($n = 144$). Means ± SEM are shown. *P*-values of 2-tailed unpaired *t*-tests are indicated (99% confidence level); ****$P < 0.0001$. b) Male fertility test of control, *mob4*^{RNAi}, *Strip*^{RNAi}, and *Cka*^{RNAi}. Germinal downregulation was achieved by crossing UAS-RNAi flies (as in a) to the nos-GAL4 driver line. Males of each genotype were individually mated with wild-type females. Data points represent numbers of progeny from individual males. Means ± SEM are shown for at least $n = 8$ males per genotype. *P*-values of 2-tailed unpaired *t*-tests are indicated (99% confidence level). c) Female fertility test of control, *mob4*^{RNAi}, *Strip*^{RNAi}, and *Cka*^{RNAi}. Germinal downregulation was achieved as in b. Females of each genotype were individually mated with wild-type males. Data points represent numbers of progeny from individual females. Means ± SEM are shown for at least $n = 9$ females per genotype. *P*-values of 2-tailed unpaired *t*-tests are indicated (99% confidence level); ****$P < 0.0001$, ns, not significant. (d–i) Whole mount testes stained with phalloidin-594 to visualize the terminal epithelium (highlighted pink) and seminal vesicles (highlighted white) in 2-day-old (d-f) and 10-day-old (g-i) control, *mob4*^{RNAi}, and *Strip*^{RNAi} unmated flies. Pink star highlights enlargement of terminal epithelium. *Strip*^{RNAi} (j) and *Cka*^{RNAi} (l) testes from 2-day-old males were immunostained with antipolyglycylated tubulin (green) to visualize spermatid axonemes. Actin cones and spermatid bundles from *Strip*^{RNAi} (k) and *Cka*^{RNAi} (m) depleted testes visualized with phalloidin-594 and immunostained to reveal polyglycylated tubulin (green).

recently found to act within the somatic lineage of the *Drosophila* male gonad, to regulate germline lineage proliferation by acting as negative regulators of JNK signaling (La Marca *et al.* 2019). Our current findings point to an additional requirement for Strip and Cka at later stages in spermiogenesis, particularly during the postmeiotic spermatid individualization. As spermiogenesis defects may be a consequence of defects occurring earlier during spermatogenesis, the use of drivers for expression in late spermatocytes would allow to clarify whether Mob4, Strip, and Cka are required specifically at spermiogenesis.

Mitochondria are known to assist axonemal growth during spermatid elongation. TEM analysis revealed unexpected defects in the mitochondrial derivatives of elongating cysts in *mob4*^{RNAi} testes. At the onset of elongation, the 2 mitochondrial derivatives extend in parallel with the growing axoneme (Regan and Fuller 1990). One of them accumulates a dense body of paracrystalline material and becomes the major mitochondrial derivative, while the other reduces in size and volume until individualization is completed. In the elongating cysts of *mob4*^{RNAi} males, it was possible to observe accumulation of paracrystalline material in both mitochondrial derivatives as also described in the *big bubble 8* mutant (Vedelek *et al.* 2016). Moreover, following *mob4*^{RNAi}, both mitochondrial derivatives often displayed irregular shapes and dimensions; a similar phenotype to that was reported for the *wampa* (*wam*) mutant (Bauerly *et al.* 2020). Wampa is a dynein subunit, and *wam* mutant spermatids lack the axonemal outer dynein arm, leading to loss of flagellar motility. It therefore seems likely that defects in axonemal organization could lead to the defects in mitochondria structure of the type we observe. However, as mitochondria provide structural and physical support for the developing axoneme, defects in mitochondrial elongation could further destabilize the developing axoneme as previously suggested (Hoyle and Raff 1990; Fuller 1993).

At present, we can only speculate about the molecular function of Mob4 in spermiogenesis. We note that clathrin heavy chain (Chc4) mutants are also defective in receptor-mediated endocytosis, neurotransmitter secretion, and spermatid individualization (Bazinet *et al.* 1993). This raises a tempting possibility of common functions for Chc4 and Mob4, particularly since Mob4 has a role in vesicular trafficking functions and shares sequence homology with the σ subunits of clathrin adaptor complexes (Baillat *et al.* 2001; Bailly and Castets 2007). Moreover, Strip has also been shown to regulate endosome trafficking and microtubule stabilization during axon elongation (Sakuma *et al.* 2014). Further studies of proteins that interact with the STRIPAK complex in the testes will be required to test these possibilities.

In summary, our present study has identified essential roles in spermatogenesis and male fertility for the Mob4, Strip, and Cka genes. Mob4 is required for proper axoneme structure, and *mob4*-depleted testes display a range of defects throughout multiple stages of sperm development. Understanding how Mob4 regulates the architecture of axonemal microtubules and how this affects other aspects of cellular function will be indispensable for understanding the pleiotropic manifestation of diseases and clinical conditions, such as sterility, that arise from the dysfunction of STRIPAK genes.

Data availability

The authors confirm that all relevant data supporting the findings of this study are available within the article and/or its supplementary information file.

Supplemental material available at GENETICS online .

Acknowledgments

Drosophila stocks obtained from the Bloomington Drosophila Stock Center (NIH P40OD018537) were used in this study. We also thank Flybase (Gramates *et al.* 2022) and FlyAtlas (Krause *et al.* 2022) for providing database information.

We acknowledge the Light Microscopy Unit of University of Algarve, partially supported by national funds through FCT under the project: PPBI-POCI-01-0145-FEDER-022122. We acknowledge support from ABC and Câmara Municipal de Loulé. We also thank Simon Collier and Alla Madich from the University of Cambridge, Department of Genetics, Fly Facility Microinjection Service for injection of the transgenic and CRISPR/Cas9 flies.

Funding

This work was funded by the Algarve 2020 Program, grant number ALG-01-0145-FEDER-030014, cofinanced by FEDER Funds through the Operational Program for Competitiveness Factors—COMPETE 2020 and by national funds through FCT—Foundation for Science and Technology under the Project PTDC/BIA-CEL/30014/2017. IBS was funded by FCT fellowship SFRH/BD/141734/2018. AW acknowledges Cancer Research UK for a PhD studentship (1999-2003). GC was funded by the Ministero dell'Istruzione, dell'Università e della Ricerca (MIUR 2020CLZ5XW). DMG acknowledges past grants from CRUK and Wellcome and current support from NIH grant R01NS119614.

Conflicts of interest

The author(s) declare no conflict of interest.

Literature cited

Arama E, Agapite J, Stell H. Caspase activity and a specific cytochrome C are required for sperm differentiation in *Drosophila*. Dev Cell. 2003;4(5):687–697. doi:10.1016/s1534-5807(03)00120-5.

Bae SJ, Ni L, Osinski A, Tomchick DR, Brautigam CA, Luo X. SAV1 promotes hippo kinase activation through antagonizing the PP2A phosphatase STRIPAK. Elife. 2017;6:e30278. doi:10.7554/eLife.30278.

Baillat G, Moqrich A, Castets F, Baude A, Bailly Y, Benmerah A, Monneron A. Molecular cloning and characterization of phocein, a protein found from the Golgi complex to dendritic spines. Mol Biol Cell. 2001;12(3):663–673. doi:10.1091/mbc.12.3.663.

Bailly Y, Castets F. Phocein: a potential actor in vesicular trafficking at Purkinje cell dendritic spines. The Cerebellum. 2007;6(4):344–352. doi:10.1080/14734220701225912.

Bauerly E, Yi K, Gibson MC. Wampa is a dynein subunit required for axonemal assembly and male fertility in *Drosophila*. Dev Biol. 2020;463(2):158–168. doi:10.1016/j.ydbio.2020.04.006.

Bazinet C, Katzen AL, Morgan M, Mahowald AP, Lemmon SK. 1993. The *Drosophila* clathrin heavy chain gene: clathrin function is essential in a multicellular organism. Genetics;134(4):1119–1134. doi:10.1093/genetics/134.4.1119

Bellen HJ, Levis RW, Liao G, He Y, Carlson JW, Tsang G, Evans-Holm M, Hiesinger PR, Schulze KL, Rubin GM, Hoskins RA, Spradling AC. 2004. The BDGP gene disruption project: single transposon insertions associated with 40% of Drosophila genes. Genet. 167(2):761–781. doi:10.1534/genetics.104.026427

Berger J, Berger S, Currie PD. Mob4-dependent STRIPAK involves the chaperonin TRiC to coordinate myofibril and microtubule network growth. PLoS Genet. 2022;18(6):e1010287. doi:10.1371/journal.pgen.1010287.

Chen HW, Marinissen MJ, Oh SW, Chen X, Melnick M, Perrimon N, Gutkind JS, Hou SX. CKA, a novel multidomain protein, regulates the JUN N-terminal kinase signal transduction pathway in *Drosophila*. Mol Cell Biol. 2002;22(6):1792–1803. doi:10.1128/MCB.22.6.1792-1803.2002.

Chen R, Xie R, Meng Z, Ma S, Guan KL. STRIPAK integrates upstream signals to initiate the hippo kinase cascade. Nat Cell Biol. 2019; 12(12):1565–1577. doi:10.1038/s41556-019-0426-y.

Chen M, Zhang H, Shi XZ, Li Y, Zhang X, Gao Z, Zhou L, Ma J, Xu Q, Guan J, *et al.* The MST4–MOB4 complex disrupts the MST1–MOB1 complex in the hippo–YAP pathway and plays a pro-oncogenic role in pancreatic cancer. J Biol Chem. 2018; 293(37):14455–14469. doi:10.1074/jbc.RA118.003279.

Couzens AL, Knight JDR, Kean MJ, Teo G, Weiss A, Dunham WH, Lin ZY, Bagshaw RD, Sicheri F, Pawson T, *et al.* Protein interaction network of the mammalian hippo pathway reveals mechanisms of kinase-phosphatase interactions. Sci Signal. 2013;6(302):rs15. doi:10.1126/scisignal.2004712.

Fabrizio J, Hime G, Lemmon S, Bazinet C. Genetic dissection of sperm individualization in *Drosophila melanogaster*. Development. 1998; 125(10):1833–1843. doi:10.1242/dev.125.10.1833.

Florindo C, Mimoso JM, Palma SL, Gonçalves C, Silvestre D, Campinho M, Tavares AA. Mob4 is required for neurodevelopment in zebrafish. MicroPublication Biol. 2023. doi:10.17912/micropub.biology.000762.

Fuller M. Spermatogenesis. In: Bate M, Arias AM, editors. The Development of Drosophila Melanogaster. NY: Cold Spring Harbor Laboratory Press; 1993. p. 71–147.

Fuller MT. Genetic control of cell proliferation and differentiation in *Drosophila spermatogenesis*. Seminars in Cell & Developmental Biology. 1998;9(4):433-444. doi:10.1006/scdb.1998.0227

Goudreault M, D'Ambrosio LM, Kean MJ, Mullin MJ, Larsen BG, Sanchez A, Chaudhry S, Chen GI, Sicheri F, Nesvizhskii AI, *et al.* A PP2A phosphatase high density interaction network identifies a novel striatin-interacting phosphatase and kinase complex linked to the cerebral cavernous malformation 3 (CCM3) protein. Mol Cell Proteomics. 2009;8(1):157–171. doi:10.1074/mcp.M800266-MCP200.

Gramates LS, Agapite J, Attrill H, Calvi BR, Crosby M, dos Santos G, Goodman JL, Goutte-Gattat D, Jenkins V, Kaufman T, *et al.* Flybase: a guided tour of highlighted features. Genetics. 2022; 220(4):iyac035. doi:10.1093/genetics/iyac035.

Gratz SJ, Ukken FP, Rubinstein CD, Thiede G, Donohue LK, Cummings AM, O'Connor-Giles KM. Highly specific and efficient CRISPR/cas9-catalyzed homology-directed repair in *Drosophila*. Genetics. 2014;196(4):961–971. doi:10.1534/genetics.113.160713.

Hoyle HD, Raff EC. Two *Drosophila* beta tubulin isoforms are not functionally equivalent. J Cell Biol. 1990;111(3):1009–1026. doi:10.1083/jcb.111.3.1009.

Hwang J, Pallas DC. STRIPAK complexes: structure, biological function, and involvement in human diseases. Int J Biochem Cell Biol. 2014;47:118–148. doi:10.1016/j.biocel.2013.11.021.

Jeong BC, Bae SJ, Ni L, Zhang X, Bai XC, Luo X. Cryo-EM structure of the hippo signaling integrator human STRIPAK. Nat Struct Mol Biol. 2021;28:290–299. doi:10.1038/s41594-021-00564-y.

Khabirova E, Moloney A, Marciniak SJ, Williams J, Lomas DA, Oliver SG, Favrin G, Sattelle DB, Crowther DC. The TRiC/CCT chaperone is implicated in Alzheimer's disease based on patient GWAS and an RNAi screen in ab-expressing *Caenorhabditis elegans*. PLoS ONE. 2014;9(7):e102985. doi:10.1371/journal.pone.0102985.

Krause SA, Overend G, Dow JAT, Leader DP. Flyatlas 2 in 2022: enhancements to the *Drosophila melanogaster* expression atlas. Nucleic Acids Res. 2022;50(D1):D1010–D1015. doi:10.1093/nar/gkab971.

La Marca JE, Diepstraten ST, Hodge AL, Wang H, Hart AH, Richardson HE, Gregory Somers W. Strip and Cka negatively regulate JNK signalling during *Drosophila* spermatogenesis. Development. 2019;146(13):dev174292. doi:10.1242/dev.174292

Lin H, Yue L, Spradling AC. The *Drosophila* fusome, a germline-specific organelle, contains membrane skeletal proteins and functions in cyst formation. Development. 1994;120(4):947–956. doi:10.1242/dev.120.4.947.

Lindsley DT, Tokuyasu KT. Spermatogenesis. In: Ashburner M, Wright TR, editors. Genetics and Biology of Drosophila. 2nd edition. New York: Academic Press; 1980. p. 225–294.

Lipinszki Z, Wang P, Grant R, Lindon C, Dzhindzhev NS, D'Avino PP, Przewloka MR, Glover DM, Archambault V. Affinity purification of protein complexes from *Drosophila* embryos in cell cycle studies. Methods Mol Biol. 2014;1170:571–588. doi:10.1007/978-1-4939-0888-2_33.

Maia T, Gogendeau D, Pennetier C, Janke C, Basto R. Bug22 influences cilium morphology and the posttranslational modification of ciliary microtubules. Biol Open. 2014;3(2):138–151. doi:10.1242/bio.20146577.

Mazo G. Quickfigures: a toolkit and ImageJ PlugIn to quickly transform microscope images into scientific figures. PLoS ONE. 2021; 16(11):e0240280. doi:10.1371/journal.pone.0240280.

Neisch AL, Neufeld TP, Hays TS. A STRIPAK complex mediates axonal transport of autophagosomes and dense core vesicles through PP2A regulation. J Cell Biol. 2017;216(2):441–461. doi:10.1083/jcb.201606082.

Noguchi T, Koizumi M, Hayashi S. Sustained elongation of sperm tail promoted by local remodeling of giant mitochondria in *Drosophila*. Curr Biol. 2011;21(10):805–814. doi:10.1016/j.cub.2011.04.016.

Regan CL, Fuller M. Interacting genes that affect microtubule function in *Drosophila melanogaster*: two classes of mutation revert the failure to complement between haync2 and mutations in tubulin genes. Genetics. 1990;125(1):77–90. doi:10.1093/genetics/125.1.77.

Rogowski K, Juge F, van Dijk J, Wloga D, Strub JM, Leviliers N, Thomas D, Bré MH, van Dorsselaer A, Gaertig J, *et al.* Evolutionary divergence of enzymatic mechanisms for posttranslational polyglycylation. Cell. 2009;137(6):1076–1087. doi:10.1016/j.cell.2009.05.020.

Sakuma C, Kawauchi T, Haraguchi S, Shikanai M, Yamaguchi Y, Gelfand VI, Luo L, Miura M, Chihara T. *Drosophila* strip serves as a platform for early endosome organization during axon elongation. Nat Commun. 2014;5(1):5180. doi:10.1038/ncomms6180.

Schneider CA, Rasband WS, Eliceiri KW. NIH image to ImageJ: 25 years of image analysis. Nat Methods. 2012;9(7):671–675. doi:10.1038/nmeth.2089.

Schulte J, Sepp K, Jorquera R, Wu C, Song Y, Hong P, Littleton T. DMob4/MOB4 regulates synapse formation, axonal transport, and microtubule organization. J Neurosci. 2010;30(15):5189–5203. doi:10.1523/JNEUROSCI.5823-09.2010.

Siddall NA, Hime GR. A *Drosophila* toolkit for defining gene function in spermatogenesis. Reproduction. 2017;153(4):121–132. doi:10.1530/REP-16-0347.

Tates AD. 1971. Cytodifferentiation during spermatogenesis in *Drosophila melanogaster*: an electron microscope study. Proefschrift, Rijksuniversiteit te Leiden.

Tokuyasu KT, Peacock WJ, Hardy RW. Dynamics of spermiogenesis in *Drosophila melanogaster*, individualization process. Z Zellforsch Mikrosk Anat. 1972;124(4):479–506. doi:10.1007/BF00335253.

Trammell MA, Mahoney NM, Agard DA, Vale RD. Mob4 plays a role in spindle focusing in *Drosophila* S2 cells. J Cell Sci. 2008;121(8):1284–1292. doi:10.1242/jcs.017210.

Tüttelmann F, Ruckert C, Röpke A. Disorders of spermatogenesis: perspectives for novel genetic diagnostics after 20 years of

unchanged routine. Medgen. 2018;30(1):12–20. doi:10.1007/s11825-018-0181-7.

Vedelek V, Laurinyecz B, Kovács AL, Juhász G, Sinka R. Testis-specific bb8 is essential in the development of spermatid mitochondria. PLoS ONE. 2016;11(8):e0161289. doi:10.1371/journal.pone.0161289.

White-Cooper H. Molecular mechanisms of gene regulation during *Drosophila* spermatogenesis. Reproduction. 2010;139(1):11–21. doi:10.1530/REP-09-0083.

Zheng Y, Liu B, Wang L, Lei H, Prieto KDP, Pan D. Homeostatic control of Hpo/MST kinase activity through autophosphorylation-dependent recruitment of the STRIPAK PP2A phosphatase Complex. Cell Rep. 2017;21(12):3612–3623. doi:10.1016/j.celrep.2017.11.076.

Editor: H. Jafar-Nejad